Improvement of time–delayed feedback control by periodic modulation: analytical theory of Floquet mode control scheme

Wolfram Just[a,b)*†] Svitlana Popovich[a)], Andreas Amann[a)], Nilüfer Baba[a)], and Eckehard Schöll[a)],

[a)] *Institut für Theoretische Physik, Technische Universität Berlin, Hardenbergstr. 36, D–10623 Berlin, Germany*

[b)] *Theoretische Physik I, TU–Chemnitz, D–09107 Chemnitz, Germany*

(December 19, 2002)

We investigate time–delayed feedback control schemes which are based on the unstable modes of the target state, to stabilise unstable periodic orbits. The periodic time dependence of these modes introduces an external time scale in the control process. Phase shifts that develop between these modes and the controlled periodic orbit may lead to a huge increase of the control performance. We illustrate such a feature on a nonlinear reaction diffusion system with global coupling and give a detailed investigation for the Rössler model. In addition we provide the analytical explanation for the observed control features.

PACS numbers: 05.45.Gg, 02.30.Ks

I. INTRODUCTION

Control of chaos is still one of the most active topics in applied nonlinear science. Despite the fact that engineers and applied mathematicians have dealt with control problems for a long time and a huge amount of knowledge has been gathered (e.g. [1–3]) some new ideas have been introduced by physicists a decade ago [4] and have boosted an enormous amount of work on control problems [5,6]. These new concepts are based on the observation that chaotic motion provides a large number of unstable states which can be stabilised by tiny control power. Thus noninvasive control schemes can be used efficiently to switch between quite different states of a single dynamical system.

Standard control schemes usually require some knowledge of the underlying dynamics, e.g. some cost function, a mathematical model of the dynamics, some costly data processing, or at least some degree of stability with respect to parameter changes. Time–delayed feedback schemes which have been developed in the wake of the above mentioned developments remove most of these constraints and can be successfully applied to stabilise time periodic states without great effort [7]. Time–delayed feedback schemes are based on the measurement of a single signal $s(t)$ and generate a control force using the time–delayed difference $s(t) - s(t-\tau)$. The delay time τ is adjusted to the period of the orbit which will be stabilised. By construction such a control force vanishes if control works successfully.

Despite its success in different experimental contexts (e.g. [8,9]) and a large number of numerical simulations that have been performed a deeper analytical understanding of time–delayed feedback control scheme has been gained just over the last few years [10,11] by performing stability analysis of the corresponding differential–difference equations. Various aspects have been clarified, e.g. the enlargement of the control domains by multiple delays [12], the limiting effect of a control loop latency [13] that has been known by engineers in the context of control theory for decades [14], and the crucial problem to adjust the delay time if the period of the orbit is not known a priori [15–17]. Meanwhile excellent reviews on chaos control problems are available [6] which cover most of these topics.

Recently the interest has shifted from low–dimensional dynamical systems to control in systems with many degrees of freedom, in particular to spatio–temporal control. Such attempts nicely demonstrate that control schemes have to be based on those eigenmodes which destabilise the state under consideration. An experimental realisation has been performed in the context of optical systems [18] where Fourier modes are the suitable modes to constitute the control scheme.

To make such a statement more explicit let us recall some basic formal features of time–delayed feedback control [10]. Let $\boldsymbol{x}(t)$ denote the internal degrees of freedom of the full dynamical system, e.g. a high–dimensional state vector. We intend to stabilise an unstable periodic state, $\boldsymbol{\xi}(t) = \boldsymbol{\xi}(t+\tau)$, by applying suitable control forces $F(t)$. Using signals $s(t) = g[\boldsymbol{x}(t)]$ which depend on the state of the system through a function g to be specified, control forces are obtained from time delayed differences $F(t) = K\,(s(t) - s(t-\tau))$. The control amplitude K which acts as

*permanent address: School of Mathematical Sciences, Queen Mary / Univ. of London, Mile End Road, London E1 4NS, UK

†e–mail: wolfram.just@physik.tu-chemnitz.de

a linear amplification is the important control parameter. The full dynamics including the control forces is governed by equations of motion

$$\dot{\boldsymbol{x}}(t) = \boldsymbol{f}(\boldsymbol{x}(t), F(t)) \quad . \tag{1}$$

Performing a linear stability analysis of eq.(1) we arrive at the Floquet eigenvalue problem [10]

$$\Lambda \boldsymbol{U}(t) + \dot{\boldsymbol{U}}(t) = D_1 \boldsymbol{f}(\boldsymbol{\xi}(t), 0)\boldsymbol{U}(t) - K(1 - \exp(-\Lambda\tau))M[\boldsymbol{\xi}(t)]\boldsymbol{U}(t), \quad \boldsymbol{U}(t) = \boldsymbol{U}(t+\tau) \tag{2}$$

where we have introduced the control matrix $M[\boldsymbol{\xi}] = -d_2 f(\boldsymbol{\xi}, 0) \otimes dg[\boldsymbol{\xi}]$ as an abbreviation. Floquet exponents Λ and Floquet eigenvectors $\boldsymbol{U}(t)$ depend on the control amplitude K, and we use the notation λ and $\boldsymbol{u}(t)$ to indicate the corresponding quantities of the uncontrolled system, $K = 0$. Since the orbit under consideration is unstable at least one of the free exponents λ has positive real part. For successful control all eigenvalues of eq.(2) must have negative real part. Such a goal depends crucially on the control matrix M which contains all the details of the coupling of the control force to the internal degrees of freedom and the properties of the signal $s(t)$.

It is quite difficult to predict the Floquet exponents of the controlled system on such a general level. But there exists one control scheme which can be treated analytically and which we call *diagonal control*. If each degree of freedom is measured and coupled to the system, such that the control matrix $M[\boldsymbol{\xi}]$ becomes the identity then the characteristic equation of the eigenvalue problem (2) reads (cf. [10])

$$\Lambda = \lambda - K(1 - \exp(-\Lambda\tau)) \quad . \tag{3}$$

Eq.(3) can be discussed by analytical methods [19] and the main results are summarised in figure 1. One typically obtains a butterfly shaped spectrum and a finite control interval bounded by flip (period doubling) and Hopf instabilities, provided the Lyapunov exponent of the uncontrolled orbit, Reλ, is not too large [20]. Strictly speaking such a shape for the Floquet eigenvalue spectrum is only valid for diagonal control. However, in terms of a perturbation expansion one can show that apart from a rescaling of the control amplitude eq.(3) remains valid [21] and that the properties of other control schemes are captured at least qualitatively.

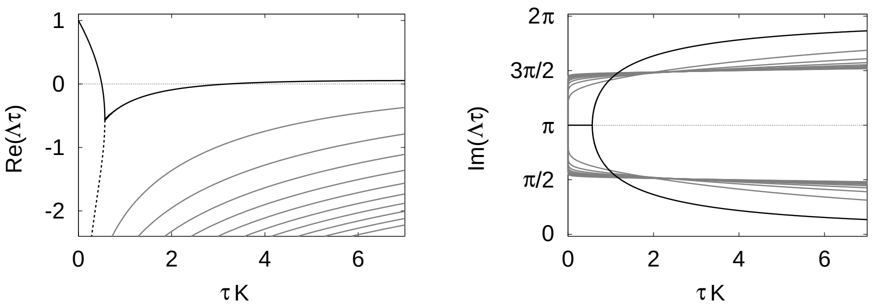

FIG. 1. Dependence of the Floquet exponents on the control amplitude according to eq.(3) for $\lambda\tau = 1 + i\pi$. Solid line: largest branch, broken/grey: nonleading branches.

From the analytical point of view diagonal control seems to be the most powerful scheme since every degree of freedom is measured and controlled. Unfortunately the scheme is difficult and often impossible to implement in real experimental situations. Thus one needs approaches which rely on less information about the state of the system. We have already mentioned that the unstable modes of the free orbit are important ingredients of a successful control scheme. Based on these objects one can construct control forces which need less measurements compared to diagonal control, which are more realistic from an experimental point of view, but which are still amenable to an analytical treatment. If $\boldsymbol{u}_\nu(t)$ denotes an unstable mode of the state we intend to stabilise then a suitable control matrix is given by $M[\boldsymbol{\xi}(t)] = \boldsymbol{u}_\nu(t) \otimes \boldsymbol{v}_\nu^*(t)$, where $\boldsymbol{v}_\nu$ denotes some suitable adjoint vector. Such a control matrix can be realised if we consider the control signal $s(t) = \langle \boldsymbol{v}_\nu(t) | \boldsymbol{x}(t) \rangle$ where $\langle . | . \rangle$ denotes an inner product, and if we couple the force $F(t)$ to the internal degrees of freedom through a Floquet eigenmode

$$\boldsymbol{f}(\boldsymbol{x}, F(t)) = \boldsymbol{f}(\boldsymbol{x}, 0) + \boldsymbol{u}_\nu(t) F(t) \quad . \tag{4}$$

A coarse inspection of eq.(2) indicates that the characteristic equation (3) is still valid (cf. section III). Thus the new scheme which just uses a single signal is as efficient as diagonal control. It generalises Fourier filtering techniques [18] to cases where translation invariance is broken so that Fourier modes no longer yield the spatial characteristics of the unstable eigenmodes.

In what follows we investigate in detail the control scheme given by eq.(4) from numerical and analytical points of view. We first illustrate the scheme by numerical simulations of a reaction diffusion system with global coupling (section II). We will show on a phenomenological level that the new scheme is even more efficient than diagonal control and that phase shifts play an important role. Such an analysis is substantiated by an analytical treatment of the control scheme (section III). We will partly solve the stability problem of the controlled system on a general level. Finally a full discussion of the stability problem and the associated Floquet spectra will be presented (section IV). Since the characteristic equations have to be solved numerically we resort for such a discussion to the Rössler model.

II. PHENOMENOLOGY OF FLOQUET MODE CONTROL

To illustrate our control method we start the investigations by looking at numerical simulations of a model system which has proven its experimental relevance in semiconductor physics. The model was originally derived for charge transport in a layered semiconductor system such as the heterostructure hot electron diode [22]. The resulting model equations are of reaction diffusion type with a global coupling. The equations in nondimensional units, including the feedback control, read

$$\begin{aligned} \partial_t u(t) &= \alpha[j_0 - (u - \langle a \rangle)] - KF_u(t) \\ \partial_t a(x,t) &= f(u-a) - Ta + \partial_x^2 a - KF_a(x,t) \quad . \end{aligned} \tag{5}$$

Here $u(t)$ is the inhibitor and $a(x,t)$ is the activator variable. In the semiconductor context $u(t)$ denotes the voltage drop across the device and $a(x,t)$ is an internal degree of freedom, e.g. an interface charge density. The local current density in the device is $j(x,t) = u(t) - a(x,t)$, and j_0 is the externally applied current which acts as a control parameter. The one–dimensional spatial coordinate x corresponds to the direction transverse to the current. We consider a system of width L with Neumann boundary conditions $\partial_x a = 0$ at $x = 0, L$ corresponding to no charge transfer through the lateral boundaries. T denotes the tunnelling rate through the collector layer. The relaxation rate α is determined by the internal and external capacitance. The global coupling represented by

$$\langle a \rangle(t) = \frac{1}{L}\int_0^L a(x,t)\, dx \tag{6}$$

arises from the application of Kirchhoff's law to the circuit in which the device is operated [23]. The nonlinear part of the transport equation, giving rise to an S–shaped local current density vs. field characteristic, is canonically modelled by a simple Lorentzian of the form

$$f(j) = j/[j^2+1] \quad . \tag{7}$$

Eqs.(5) contain control forces F_a and F_u for stabilising time periodic patterns. A variety of different choices are possible, cf. e.g. [24] for a discussion of different schemes. In the semiconductor context these forces can be implemented by appropriate electronic circuits [25].

Throughout our investigations we consider a parameter regime ($T = 0.05$, $\alpha = 0.035$, $L = 40$ and $j_0 = 1.262$) where the motion without control forces exhibits chaotic sequences of single spatio–temporal spikes pinned at one boundary. The chaotic spiking which corresponds to flashing current filaments in a semiconductor context arises via a period doubling scenario [25]. Thus unstable periodic patterns are embedded in the chaotic attractor which typically develop a single unstable Floquet mode and where the corresponding Floquet multiplier $\exp(\lambda\tau)$ is negative. Although the full set of equations of motion is a spatio-temporal system, the dynamics is essentially low–dimensional since it relaxes to a low–dimensional inertial manifold. Such a feature of course depends on boundary conditions and in particular on the size of the system, and is characteristic for globally coupled systems.

The most efficient control method might be expected to be diagonal control, which means in case of our spatially extended system that each variable is measured and controlled locally. It corresponds to the control forces

$$F_u(t) = u(t) - u(t-\tau), \quad F_a(x,t) = a(x,t) - a(x,t-\tau) \quad . \tag{8}$$

Although the scheme is quite effective it is almost impossible to be implemented in real experiments. Nevertheless it proves to be quite useful in numerical simulations and it can be used as a reference scheme since all its properties can be described analytically be the characteristic equation (3). Our model exhibits a periodic state $a_p(x,t) = a_p(x,t+\tau)$, $u_p(t) = u_p(t+\tau)$ with period $\tau = 985.9$. Using the control scheme (8) with an appropriate value of the control amplitude K the spiking becomes regular (cf. figure 2)

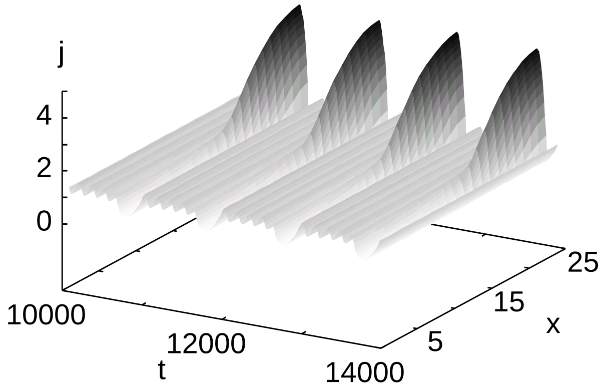

FIG. 2. Space time plot of the current $j(x,t)$ for time periodic spiking, stabilised by time–delayed feedback control.

Experimentally accessible control schemes cannot be based on diagonal control. But in general it is impossible to understand the performance of other time delayed feedback schemes on an analytical level. There are, however, a few exceptions. Following the ideas of [26] we base controls schemes on the unstable modes of the pattern which we intend to stabilise. Let $(\psi_u(t), \psi_a(x,t))$ denote the unstable Floquet eigenmode of the state $(u_p(t), a_p(x,t))$ and $(\varphi_u(t), \varphi_a(x,t))$ the eigenmode of the corresponding adjoint problem (cf. section III for formal definitions). For the control force we propose

$$\begin{aligned} F_u(t) &= K\left(\psi_u(t)s(t) - \psi_u(t-\tau)s(t-\tau)\right) \\ F_a(x,t) &= K\left(\psi_a(x,t)s(t) - \psi_a(x,t-\tau)s(t-\tau)\right) \end{aligned} \tag{9}$$

where the signal $s(t)$ is determined by the product of the state and the adjoint eigenmode

$$s(t) = \varphi_u(t)u(t) + \int \varphi_a(x,t)a(x,t)\,dx \quad . \tag{10}$$

The force (9) is based on the measurement of a single signal, and the mode $(\varphi_u(t), \varphi_a(x,t))$ plays the role of a spatio–temporal filter for the internal degrees of freedom. The coupling of the control force to the internal dynamics is mediated by the unstable Floquet eigenmode $(\psi_u(t), \psi_a(x,t))$.

The control scheme eqs.(9) and (10) is a straightforward generalisation of Fourier control. If one considers systems which are translational invariant then the spatial structure of the eigenmodes is given by plane waves. Then our scheme reduces to Fourier control [18]. However, our concept takes properly into account all effects which break translation invariance, i.e. boundary conditions or the details of the spatio-temporal pattern which we intend to stabilise. The actual eigenmodes can be computed straightforwardly from the corresponding eigenvalue problem. Figure 3 displays the spatio-temporal characteristics of the unstable eigenmode of our model. While the Floquet right–eigenmode displays spatio–temporal oscillations the adjoint left–eigenmode shows sharp spatio–temporal spiking with an amplitude that is several orders of magnitude larger than the background.

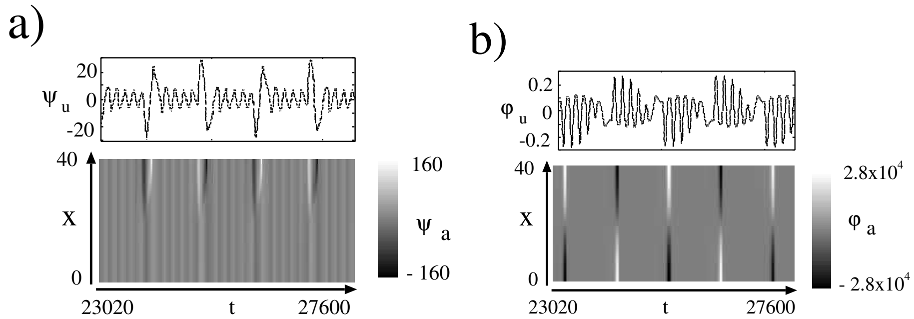

FIG. 3. (a) Floquet right–eigenmode $\psi_u(t)$ and $\psi_a(x,t)$. for the largest Floquet exponent, (b) corresponding adjoint left–eigenmode $\varphi_u(t)$ and $\varphi_a(x,t)$. Eigenmodes are computed for the state displayed in figure 2, left– and right eigenmodes are normalised to one.

We add two technical remarks. Floquet modes are of course only defined up to some normalisation constant. In order to compare the control scheme eqs.(9) and (10) and in particular the values of the control amplitude K to diagonal control we take eigenmodes which are normalised to one (cf. section III for the formal details). Furthermore eigenmodes are usually complex valued since the corresponding Floquet exponents are complex numbers. In general one has to take the real and imaginary part of the mode separately into account to obtain a real valued control force. Here we are dealing with a flip orbit where the imaginary part of the Floquet exponent is given by π/τ. Then the corresponding eigenmodes are a product of a real valued factor and a complex phase given by $\exp(i\pi t/\tau)$. Such a phase drops from our control scheme (9) and (10) and we just take the real valued factor of the modes to construct the control force. Since the full eigenmodes are periodic with period τ the real valued factors are antiperiodic, i.e. periodic with period 2τ, as it is obvious from figure 3.

A naive view suggests that Floquet mode control is as efficient as diagonal control provided only a single unstable mode triggers the instability of the pattern. We test this conjecture numerically by comparing the control performance of diagonal control (8) and of Floquet mode control eqs.(9) and (10). For our simulations we take a fixed initial condition in the vicinity of the unstable periodic orbit to exclude effects which are related to initial conditions and basins of attraction. By changing K we observe that a finite control interval appears, just in accordance with the analytical result eq.(3) (cf. figure 4). But for Floquet mode control the interval is enlarged by 6 orders of magnitude. It is in fact surprising that Floquet mode control and diagonal control differ at all.

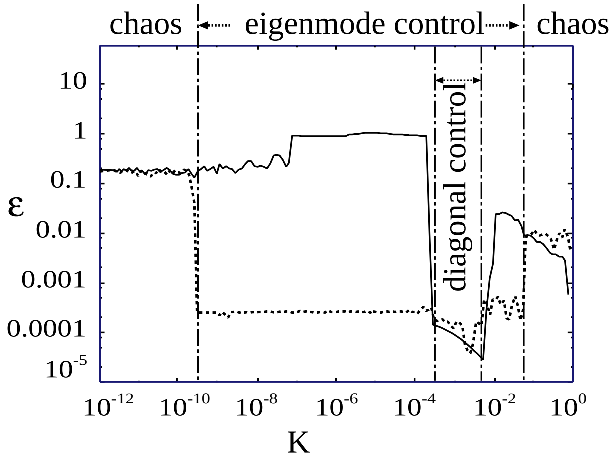

FIG. 4. Regime of Floquet eigenmode control (dotted line) and diagonal control (full line). The spatio–temporal average $\varepsilon = \langle |a(x,t) - a(x,t-\tau)| + |u(t) - u(t-\tau)| \rangle_{x,t}$ is plotted versus the control amplitude K as a measure of successful control.

The difference in the control performance can be attributed to an essential degree of freedom which we missed in the previous reasonings. Our system without control is autonomous. Thus the phase of the periodic orbit is not fixed at all and orbits $(u_p(t+\delta), a_p(x,t+\delta))$ with arbitrary value of δ yield a periodic solution. If we apply the time–delayed feedback control the control force vanishes at these states, and every solution is a candidate for successful control. For the diagonal scheme the phase δ does not matter since stability is governed by the characteristic equation (3). The final value of the phase only depends on the initial condition. But Floquet mode control introduces an additional time scale through the Floquet modes. Thus the system subjected to control is not autonomous and the stability of the periodic pattern may depend on the value of the phase shift δ. If the phase shift vanishes then stability is still governed by eq.(3) like for diagonal control. But the system may develop a finite phase shift during the control process which then leads to a different control performance as it was observed in figure 4.

Our simulations confirm such a kind of conjecture. We have measured the time dependence of the stabilised orbit and compared it with the time dependence of the Floquet modes. In order to visualise the phase difference we display the stabilised orbit and the periodic orbit which was used to determine the Floquet modes (cf. figure 5). A phase difference is clearly visible if we consider control amplitudes outside of the diagonal control interval.

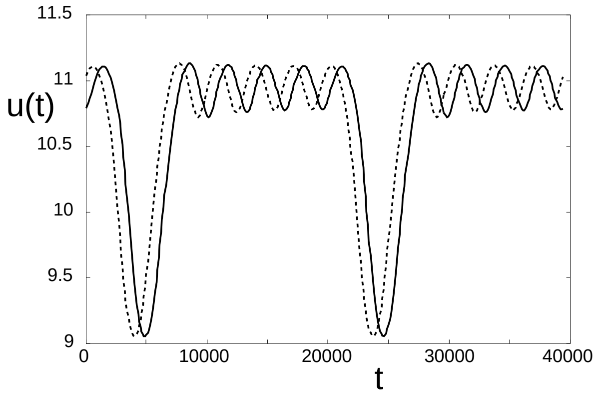

FIG. 5. Time dependence of the voltage $u(t)$ for the periodic orbit stabilised with Floquet mode control at $K = 10^{-7}$ (solid line) and for the periodic orbit used for computing the Floquet modes (broken line).

In addition these data allow to measure the dependence of the observed phase difference on the control amplitude in the whole control interval (cf. figure 6). We clearly see that a finite phase difference develops if we leave the control interval of diagonal control. Thus Floquet mode control uses the freedom to adjust the phase of the orbit properly so that a wider control interval is obtained. Similar types of resonance–like phenomena are quite common in time–delayed feedback control or more general differential–difference equations [27,28]. They have been used for different purposes in the past, e.g. for stabilising periodic orbits without torsion [29].

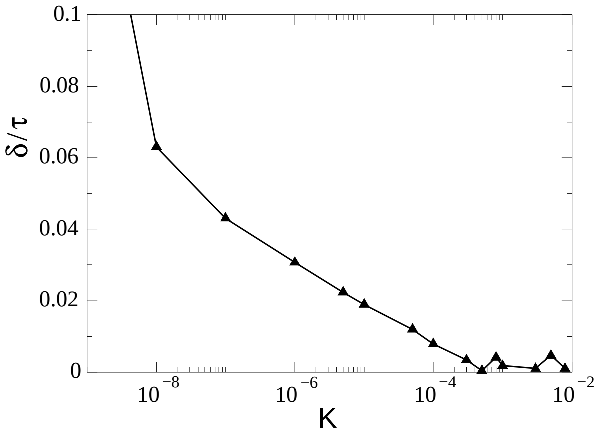

FIG. 6. Observed phase difference for Floquet mode control in dependence on the control amplitude.

III. ANALYTICAL TREATMENT OF CONTROL PROPERTIES

Our previous simulations have already shown that phase shifts between the orbit and the controller are a mechanism for the improved performance of Floquet mode control. A better understanding of this mechanism calls for analytical investigations. For that purpose we consider a general dynamical system where the internal state of the system is described by a state vector $\boldsymbol{x}(t)$. It obeys the equation of motion

$$\dot{\boldsymbol{x}}(t) = \boldsymbol{f}(\boldsymbol{x}(t)) \quad . \tag{11}$$

We suppose that eq.(11) admits a periodic orbit $\boldsymbol{\xi}(t) = \boldsymbol{\xi}(t+\tau)$. Its stability is determined by the associated Floquet eigenvalue problem

$$\lambda_\nu \boldsymbol{u}_\nu(t) + \dot{\boldsymbol{u}}_\nu(t) = D\boldsymbol{f}(\boldsymbol{\xi}(t))\boldsymbol{u}_\nu(t), \quad \boldsymbol{u}_\nu(t) = \boldsymbol{u}_\nu(t+\tau) \quad . \tag{12}$$

Here$D\boldsymbol{f}$ denotes the linearisation of the full equation of motion and Floquet exponents λ_ν are as usually restricted to a single Brillouin zone, e.g. $\mathrm{Im}\lambda_\nu \in (-\pi/\tau, \pi/\tau]$. The corresponding adjoint eigenvalue equation reads

$$\lambda_\nu \boldsymbol{v}_\nu^\dagger(t) - \dot{\boldsymbol{v}}_\nu^\dagger(t) = \boldsymbol{v}_\nu^\dagger(t) D\boldsymbol{f}(\boldsymbol{\xi}(t)), \quad \boldsymbol{v}_\nu(t) = \boldsymbol{v}_\nu(t+\tau) \quad . \tag{13}$$

The original eigenvectors $\boldsymbol{u}_\nu$ and their adjoints $\boldsymbol{v}_\nu^\dagger$ constitute a biorthogonal set and we adopt the normalisation according to the Kronecker symbol

$$\langle \boldsymbol{v}_\mu(t)|\boldsymbol{u}_\nu(t)\rangle = \boldsymbol{v}_\mu^\dagger(t)\boldsymbol{u}_\nu(t) = \delta_{\mu\nu} \quad . \tag{14}$$

We concentrate on the simplest cases, i.e. a periodic orbit with a single unstable eigenmode. Let λ_+ denote the exponent with positive real part whereas all the other exponents λ_ν $(\nu \neq +)$ have negative real part. Since torsion is an essential ingredient for time delayed feedback methods to work at all [10,11] the unstable exponent must have a finite imaginary part. Two generic cases are possible, a complex conjugate pair or a single exponent on the boundary of the Brillouin zone, $\lambda_+ = \mathrm{Re}\lambda_+ + i\pi/\tau$. Here we deal with the latter case, since it corresponds to unstable periodic orbits which have been generated in period doubling bifurcations. Since the unstable Floquet exponent is complex valued the corresponding eigenmodes $\boldsymbol{u}_+(t)$ and $\boldsymbol{v}_+(t)$ are complex valued as well. For our case of a flip orbit these modes can be written as $\boldsymbol{u}_+(t) = \exp(i\pi t/\tau)\hat{\boldsymbol{u}}_+(t)$ and $\boldsymbol{v}_+(t) = \exp(i\pi t/\tau)\hat{\boldsymbol{v}}_+(t)$ with real valued but antiperiodic factors $\hat{\boldsymbol{u}}_+(t) = -\hat{\boldsymbol{u}}_+(t+\tau)$ and $\hat{\boldsymbol{v}}_+(t) = -\hat{\boldsymbol{v}}_+(t+\tau)$.

In order to stabilise the periodic orbit $\boldsymbol{\xi}(t)$ we implement a time–delayed feedback loop which is based on a filter function $\boldsymbol{w}(t)$ and on the unstable eigenmode $\boldsymbol{u}_+(t)$

$$\dot{\boldsymbol{x}}(t) = f(\boldsymbol{x}(t)) - K\left[\boldsymbol{u}_+(t)\langle \boldsymbol{w}(t)|\boldsymbol{x}(t)\rangle - \boldsymbol{u}_+(t-\tau)\langle \boldsymbol{w}(t-\tau)|\boldsymbol{x}(t-\tau)\rangle\right] \quad . \tag{15}$$

For instance we may chose for the filter the adjoint eigenmode $\boldsymbol{w}(t) = \boldsymbol{v}_+(t)$ but we do not restrict our analysis to such a special choice. Since the eigenmodes are complex valued eq.(15) would not make sense without any comment. If we demand that the filter is real up to a complex phase factor, i.e. $\boldsymbol{w}(t) = \exp(i\pi t/\tau)\hat{\boldsymbol{w}}(t)$ then the control loop is indeed real valued and it can be written in various ways

$$\begin{aligned} &\boldsymbol{u}_+(t)\langle \boldsymbol{w}(t)|\boldsymbol{x}(t)\rangle - \boldsymbol{u}_+(t-\tau)\langle \boldsymbol{w}(t-\tau)|\boldsymbol{x}(t-\tau)\rangle = \boldsymbol{u}_+(t)\left[\langle \boldsymbol{w}(t)|\boldsymbol{x}(t)\rangle - \langle \boldsymbol{w}(t-\tau)|\boldsymbol{x}(t-\tau)\rangle\right] \\ &= \hat{\boldsymbol{u}}_+(t)\langle \hat{\boldsymbol{w}}(t)|\boldsymbol{x}(t)\rangle - \hat{\boldsymbol{u}}_+(t-\tau)\langle \hat{\boldsymbol{w}}(t-\tau)|\boldsymbol{x}(t-\tau)\rangle = \hat{\boldsymbol{u}}_+(t)\left[\langle \hat{\boldsymbol{w}}(t)|\boldsymbol{x}(t)\rangle + \langle \hat{\boldsymbol{w}}(t-\tau)|\boldsymbol{x}(t-\tau)\rangle\right] \quad . \end{aligned} \tag{16}$$

Thus our control scheme is in fact a time delayed feedback scheme based on a real valued scalar signal $s(t) = \langle \hat{\boldsymbol{w}}(t)|\boldsymbol{x}(t)\rangle$. In order to avoid a heavy notation we just stick to the notation used in eq.(15).

The control loop introduces an explicit time dependence into eq.(15). Thus the system is not any longer time translation invariant. Nevertheless an orbit $\boldsymbol{\xi}(t+\delta)$ with arbitrary phase δ is a periodic state of the controlled system, since the control force vanishes on such a special trajectory. We investigate the stability of the orbit in terms of a linear analysis. Observing the time evolution of small increments $\delta\boldsymbol{x}(t) = \boldsymbol{x}(t) - \boldsymbol{\xi}(t+\delta)$ we get a linear differential–difference equation which is solved by the usual exponential form $\delta\boldsymbol{x}(t) = \exp(\Lambda t)\boldsymbol{U}(t)$. The Floquet exponents Λ and the eigenmodes $\boldsymbol{U}$ are determined by the eigenvalue equation (cf. e.g. the approaches used in [10])

$$\Lambda\boldsymbol{U}(t) + \dot{\boldsymbol{U}}(t) = D\boldsymbol{f}(\boldsymbol{\xi}(t))\boldsymbol{U}(t) - K(1-\exp(-\Lambda\tau))\boldsymbol{u}_+(t-\delta)\langle \boldsymbol{w}(t-\delta)|\boldsymbol{U}(t)\rangle, \quad \boldsymbol{U}(t) = \boldsymbol{U}(t+\tau) \quad . \tag{17}$$

In order to simplify subsequent considerations we have introduced a new time scale $\bar{t} = t + \delta$ for writing down eq.(17). But for simplicity of the notation we omit the bar. In formal terms the solution of the eigenvalue problem (17) is quite simple. Let us define functions $\Gamma_\delta^{(\mu)}[\kappa]$ to be the Floquet exponents of the auxiliary time–delayed Floquet problem (cf. [30] for general properties of time delayed Floquet problems)

$$\Gamma_\delta^{(\mu)}[\kappa]\boldsymbol{Q}_\delta^{(\mu)}(t) + \dot{\boldsymbol{Q}}_\delta^{(\mu)}(t) = D\boldsymbol{f}(\boldsymbol{\xi}(t))\boldsymbol{Q}_\delta^{(\mu)}(t) - \kappa\boldsymbol{u}_+(t-\delta)\langle \boldsymbol{w}(t-\delta)|\boldsymbol{Q}_\delta^{(\mu)}(t)\rangle, \quad \boldsymbol{Q}_\delta^{(\mu)}(t) = \boldsymbol{Q}_\delta^{(\mu)}(t+\tau) \quad . \tag{18}$$

The index μ numbers the different exponents, the subscript δ indicates the dependence on the phase, and the argument κ is just the independent variable. Then by comparison the characteristic equation of eq.(17) reads

$$\Lambda = \Gamma_\delta^{(\mu)}[K(1-\exp(-\Lambda\tau))] \quad . \tag{19}$$

Eq.(19) is still an exact expression, but we need to compute the function appearing on the right hand side. We already see on such a general level that stability of the state may depend on the phase since δ enters the characteristic equation explicitly.

We are left with computing the functions $\Gamma_\delta^{(\mu)}[\kappa]$ from eq.(18). Let us first consider the simplest case, $\delta = 0$. Here a complete analytic solution is available (cf. appendix A). It reads

$$\Gamma_{\delta=0}^{(\nu)}[\kappa] = \lambda_\nu, \quad (\nu \neq +) \tag{20}$$

$$\Gamma_{\delta=0}^{(+)}[\kappa] = \lambda_+ - \chi\kappa \tag{21}$$

where

$$\chi = \frac{1}{\tau} \int_0^\tau \langle \boldsymbol{w}(t) | \boldsymbol{u}_+(t) \rangle \, dt \quad . \tag{22}$$

Eq.(20) shows, that the stable branches of the uncontrolled system do not contribute to the stability features of the controlled orbit. The characteristic equation arising from the unstable branch (cf. eqs.(19) and (21)) coincides with the corresponding expression of diagonal control (cf. eq.(3)) apart from a linear rescaling of the control amplitude by the parameter (22). Thus for in–phase orbits Floquet mode control is as efficient as diagonal control. Above all the results are almost independent of the choice of the filter $\boldsymbol{w}(t)$, i.e. independent from the measured signal. It is the coupling of the force to the internal degrees of freedom via the unstable mode which plays the crucial role here.

We now dwell on the out–of–phase orbits, i.e. on the stability problem for $\delta \neq 0$. Apparently there does not exist a closed analytical solution for $\Gamma_\delta^{(\mu)}[\kappa]$. Only periodicity $\Gamma_\delta^{(\mu)}[\kappa] = \Gamma_{\delta+\tau}^{(\mu)}[\kappa]$ which results from the periodicity of the orbit is obvious from eq.(18). Thus we are bound to perturbative approaches. Since the solutions which are related to stable branches of the uncontrolled system do not play any role for $\delta = 0$ we restrict ourselves to the case $\mu = +$, i.e. to the branch which connects to λ_+. The corresponding characteristic equation reads

$$\Lambda = \Gamma_\delta^{(+)}[K(1 - \exp(-\Lambda\tau))], \quad \Gamma_\delta^{(+)}[0] = \lambda_+ \quad . \tag{23}$$

In particular we are interested in the critical control amplitudes which limit the control interval (cf. e.g. figure 1). At the lower boundary the interval is limited by a flip bifurcation, i.e. the corresponding control amplitude $K = K_{\mathrm{fl}}(\delta)$ is determined by the condition $\Lambda = i\pi/\tau$. Hence eq.(23) results in

$$i\pi/\tau = \Gamma_\delta^{(+)}[2K_{\mathrm{fl}}(\delta)] \quad . \tag{24}$$

To determine the sensitivity of the control threshold on the phase shift we take the derivative with respect to δ and get (cf. appendix A)

$$\partial_\delta K_{\mathrm{fl}}(\delta) = -A(\delta) K_{\mathrm{fl}}(\delta) \quad . \tag{25}$$

Whenever the coefficient $A(\delta)$ is positive we obtain an exponential decrease of the control amplitude,

$$K_{\mathrm{fl}}(\delta) \simeq K_{\mathrm{fl}}(0) \exp(-\int A(\delta) d\delta) \tag{26}$$

i.e. an increase of the control interval which is quite sensitive on the phase shift (cf. the simulations of section II). For small δ and the special choice $\boldsymbol{w}(t) = \boldsymbol{v}_+(t)$ we obtain $K_{\mathrm{fl}}(\delta) \simeq K_{\mathrm{fl}}(0) \exp(-A_0\delta^2)$ with constant A_0 (cf. Appendix A).

A similar estimate can be formulated for the upper control boundary which is governed by a Hopf instability. But in order to get quantitative results we have to solve the full eigenvalue problem (23). Such an analysis has to resort to numerical approaches, which we are going to supply in the next section for a simple model system.

IV. NUMERICAL EVALUATION FOR THE RÖSSLER MODEL

A more detailed investigation of our control scheme calls for a quantitative evaluation of the stability problem associated with the characteristic equation (19). That can be done only by numerical computation of the right hand side. For such a task our original model (5) is far too complicated. Since we focus on the principal aspects of Floquet mode control we choose for the purpose of illustration the Rössler equations

$$\begin{aligned}
\dot{x}_1 &= -x_2 - x_3 - K u_1(t)[s(t) - s(t-\tau)] \\
\dot{x}_2 &= x_1 + a x_2 - K u_2(t)[s(t) - s(t-\tau)] \\
\dot{x}_3 &= b + x_1 x_3 - c x_3 - K u_3(t)[s(t) - s(t-\tau)]
\end{aligned} \tag{27}$$

with parameter values $a = 0.2$, $b = 0.2$, $c = 5.7$. We are focusing on the periodic orbit with period $\tau = 11.75863$. The unstable Floquet exponent is given by $\mathrm{Re}\lambda = 0.10684$ and $(u_1(t), u_2(t), u_3(t))$ and $(v_1(t), v_2(t), v_3(t))$ denote the Floquet right–eigenmode and the solution of the adjoint problem, respectively. The time–delayed control force is derived from the signal

$$s(t) = \langle v(t)|x(t)\rangle = \sum_{k=1}^{3} v_k^*(t)x_k(t) \quad . \tag{28}$$

We recall that the control force is real valued and can be written in various ways (cf. eq.(16)).

The control performance is governed by the Floquet spectra, which are determined by the stability problem (17) and the characteristic equation (19), respectively. We use a Benettin algorithm [31] for the numerical computation of the Floquet exponents. Such an algorithm can be applied easily to obtain the leading part of the eigenvalue spectrum, since one just requires the forward integration of the linearised equation and successive reorthogonalisation. The algorithm yields the real parts of the exponents, ReΛ, since it detects the expansion in phase space but ignores the torsion. Results are displayed in figure 7. We observe the typical butterfly shaped behaviour which is already known from our analytical investigations (cf. figure 1). On increasing the phase shift the spectrum first moves upwards and apparently the size of the control interval decreases.

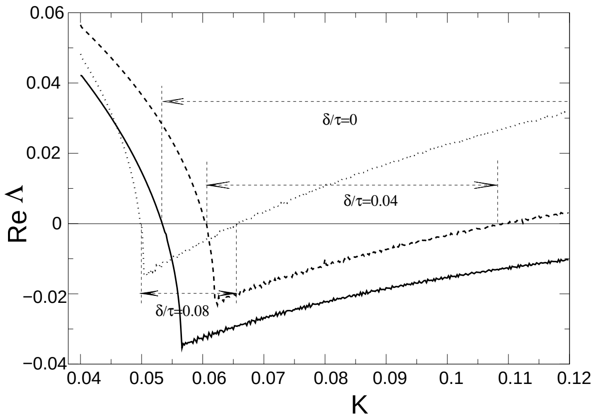

FIG. 7. Largest Floquet exponent of the controlled Rössler system in dependence on the control amplitude for different values of the phase shift: $\delta = 0$ (solid), $\delta = 0.04\tau$ (dashed), $\delta = 0.08\tau$ (dotted). Arrows indicate the control interval. The trivial exponent $\Lambda = 0$ is not displayed.

The Floquet spectra clearly show that the control interval depends sensitively on the phase shift. To reveal such a dependence of the control boundaries let us evaluate the lower control boundary using eq.(24). For numerical purposes we introduce the Floquet multiplier $z = \exp(\Lambda\tau)$ so that the characteristic equation (19) is given by

$$0 = \det(1 - z^{-1}W_{z^{-1}}(\tau)) \tag{29}$$

where we have introduced the evolution matrix of the controlled system via

$$\dot{W}_{z^{-1}}(t) = \left[D\boldsymbol{f}(\boldsymbol{\xi}(t)) - K(1 - z^{-1})\boldsymbol{u}_+(t-\delta) \otimes \boldsymbol{w}(t-\delta)\right] W_{z^{-1}}(t), \quad W_{z^{-1}}(0) = 1 \quad . \tag{30}$$

Eq.(30) is very convenient for numerical computation of the spectrum (cf. [32]). Here we are interested in the lower critical control amplitude $K_{\mathrm{fl}}(\delta)$. Thus we fix $z = -1$ (cf. eq.(24)) and solve numerically eq.(29) for K. The results are displayed in figure 8. We observe a quite complicated dependence of the threshold on the phase shift. $K_{\mathrm{fl}}(\delta)$ is of course periodic in δ with period τ. For small phase shift the threshold increases so that the threshold has a local minimum at $\delta = 0$. The corresponding quadratic dependence on δ is in accordance with our perturbative results (cf. appendix A). For intermediate values of the phase shift the threshold lowers and there is a pronounced region of bistability where stable in–phase and certain out–of–phase orbits coexist. In addition, the orbit is stable even below the threshold of diagonal control for certain phase shifts. Whether such linearly stable states are reached during the control process depends of course on the basin of attraction of these states.

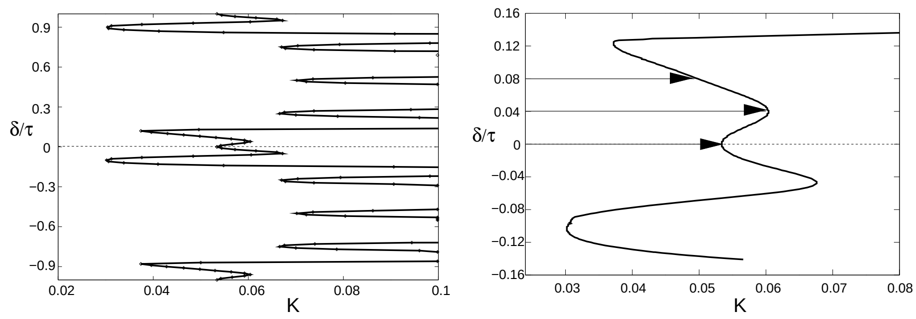

FIG. 8. Dependence of the lower control threshold $K = K_{\mathrm{fl}}$ on the phase shift δ. Left: Dependence over two complete periods $\delta \in [-\tau, \tau]$. Right: Enlarged section for small phase shift. Arrows indicate parameters used for the spectra in figure 7.

The evaluation and even the visualisation of global properties of differential–difference equations is a complicated task since the phase space is infinite–dimensional. Thus one cannot expect to get a complete overview of the basin of attraction for the orbit under consideration. Nevertheless we go beyond linear stability analysis and compute for different initial conditions which phase shift develops during the control process. In order to capture our essential degree of freedom, namely the phase, we choose a fixed initial condition in a reference frame that is shifted in time by δ, $\bar{t} = t + \delta$ (cf. section III). Thus the phase shift enters the control matrix as a parameter and we can study the influence of different phase–shifted initial conditions just be sweeping this external parameter in our simulation. We compute the asymptotic state by neglecting a transient of length $t = 470\tau$. The value of the control force at integer multiples of the period is displayed in figure 9 in dependence on K. In each case we observe a finite control interval where the control signal displays a finite jump at the lower boundary. Thus the corresponding bifurcation is subcritical. Beyond the instability the solution locks to a period–two state[1] which then undergoes a period doubling sequence on lowering K further. For $\delta = 0$ the control boundary coincides with the results of the linear stability analysis (cf. figure 7). For initial condition with phase shift $\delta = 0.04\tau$ we obtain essentially the same control interval. Thus in the control region where the phase shifted orbit is linearly unstable the phase of the initial condition drifts during the control process and locks to the state $\delta = 0$ which is linearly stable. We have already found such a feature in the simulations of the reaction–diffusion model (cf. figure 6). If we chose initial conditions with even larger phase shifts, $\delta = 0.08\tau$, we enter a regime where the linearly stable control interval covers control amplitudes where the in–phase orbit is unstable. Thus control extends beyond the threshold of diagonal control. These states are not accessible from an initial condition without phase shift, $\delta = 0$, since they cannot be reached continuously through a sequence of linearly stable orbits (cf. figure 8). Whenever the orbit becomes linearly unstable and no nearby stable orbit exists, the trajectory locks to the period–two state which is not a proper orbit of the uncontrolled system. Thus figure 8 gives us a hint which state is accessible during the control process from a certain initial condition.

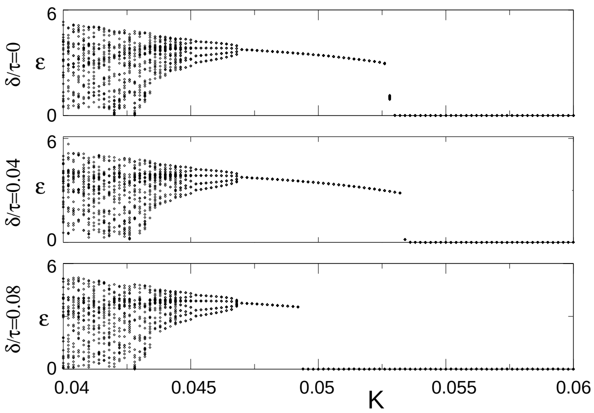

[1]Since the controlled system is non autonomous the period of the period–two state is given by 2τ. Thus $\boldsymbol{x}(t) - \boldsymbol{x}(t-\tau) = -(\boldsymbol{x}(t+\tau) - \boldsymbol{x}(t))$ and $\varepsilon(t) = \|\boldsymbol{x}(t) - \boldsymbol{x}(t-\tau)\| = \|\boldsymbol{x}(t+\tau) - \boldsymbol{x}(t)\| = \varepsilon(t+\tau)$.

FIG. 9. Control signal $\varepsilon(t)=\sum_{i=1}^{3}|x_i(t)-x_i(t-\tau)|$ at times $t=n\tau$, $0\leq n\leq 30$ in dependence on the control amplitude K for different values of the phase δ of the initial condition.

V. CONCLUSION

Time–delayed feedback methods are very useful for controlling unstable time periodic states. Since the original scheme is based on the measurement of a single variable the control can be applied in principle in quite different experimental situations. It is however difficult to estimate how the properties of the measured signal and the coupling of the control force to the internal degrees of freedom affect the performance of the control. Such questions are usually addressed by control theory for non time–delayed feedback schemes. Here we proposed a coupling scheme which is based on the unstable modes of the target state. A partial analytical treatment of the corresponding time–delayed control problem, and numerical simulations of two different model systems have been presented. More research going beyond this work would be desirable to investigate how such a scheme can be directly implemented experimentally.

The Floquet eigenmodes play a double role. On the one hand the unstable mode mediates the coupling of the control force to the internal degrees of freedom. On the other hand the adjoint mode yields a suitable filter which generates a signal from which the control force is derived. Since these modes inherit an explicit time dependence the control loop breaks the time translation invariance. Therefore the phase of the unstable periodic orbit, which is an independent variable in the uncontrolled autonomous system may adjust properly and may increase the control performance. Such a phenomenon resembles synchronisation mechanisms, although no phase locking has been found.

We have illustrated the increase of control performance by stabilizing spatio-temporal patterns in a nonlinear reaction–diffusion system. We observed an enhancement of control efficiency by several orders of magnitude. In addition we have been able to explain the basic features in analytical terms. In particular, our approach predicts a superexponential increase of the control interval (cf. [26] and appendix A).

Our analytical approach indicates that several features are independent of the particular choice of the coupling and the filter function. For instance, all properties of the in–phase orbit, i.e. control without phase shift, are independent of the filter $\boldsymbol{w}(t)$ provided that the coupling of the force to the internal degrees of freedom is mediated by the unstable Floquet eigenmode. Our analysis is in fact symmetric between the eigenmode and its adjoint. Therefore, the control performance of in–phase orbits does not depend on the coupling to the internal degrees of freedom provided we generate a signal $s(t)$ through the adjoint eigenmode. Thus our results do not depend on all the details of the eigenmodes, and an experimental implementation of our control idea seems to be feasible. In fact, we have observed in our simulations that the increase of the control performance persists if we change the filter functions used in section II.

There remains the general problem how to adjust the measured signal and the coupling to the internal degrees of freedom in order to optimise the control performance of time–delayed feedback control. Our scheme just gives a partial answer to this question. The free phase may adjust during the control process to give a better adaptation of the filter and the coupling functions. Of course our analysis is constrained to the linear regime. Global features like basins of attraction are still out of reach, and would in any case be difficult to visualize in high–dimensional phase spaces which are related with the dynamics of differential–difference equations.

ACKNOWLEDGEMENT

The authors gratefully acknowledge support by the "Deutsche Forschungsgemeinschaft" in the framework of Sfb 555 and through grant no. JU261/3-1.

APPENDIX A: ANALYTICAL PROPERTIES OF FLOQUET PROBLEMS

In order to determine $\Gamma^{(\mu)}_{\delta=0}[\kappa]$ we consider eq.(18) for $\delta=0$. Multiplication with an adjoint eigenmode $\boldsymbol{v}_\nu(t)$ yields, taking eqs.(13) and (14) into account,

$$\Gamma^{(\mu)}_{\delta=0}[\kappa]\langle \boldsymbol{v}_\nu(t)|\boldsymbol{Q}^{(\mu)}_{\delta=0}(t)\rangle+\frac{d}{dt}\langle \boldsymbol{v}_\nu(t)|\boldsymbol{Q}^{(\mu)}_{\delta=0}(t)\rangle=\lambda_\nu\langle \boldsymbol{v}_\nu(t)|\boldsymbol{Q}^{(\mu)}_{\delta=0}(t)\rangle-\delta_{\nu,+}\kappa\langle \boldsymbol{w}(t)|\boldsymbol{Q}^{(\mu)}_{\delta=0}(t)\rangle \quad . \tag{A1}$$

If we consider $\nu\neq+$ then we obtain

$$\left(\Gamma^{(\mu)}_{\delta=0}[\kappa]-\lambda_\nu\right)\langle \boldsymbol{v}_\nu(t)|\boldsymbol{Q}^{(\mu)}_{\delta=0}(t)\rangle+\frac{d}{dt}\langle \boldsymbol{v}_\nu(t)|\boldsymbol{Q}^{(\mu)}_{\delta=0}(t)\rangle=0 \quad . \tag{A2}$$

Since the inner product is by definition periodic in time eq.(A2) tells us that either the inner product or the bracket on the left hand side vanishes. Hence we obtain eq.(20), and all exponents but one are determined. Choosing $\nu = +$ eq.(A1) yields

$$\left(\Gamma^{(+)}_{\delta=0}[\kappa] - \lambda_+\right) \langle \boldsymbol{v}_\nu(t)|\boldsymbol{Q}^{(+)}_{\delta=0}(t)\rangle + \frac{d}{dt}\langle \boldsymbol{v}_\nu(t)|\boldsymbol{Q}^{(+)}_{\delta=0}(t)\rangle = -\kappa\langle \boldsymbol{w}(t)|\boldsymbol{Q}^{(+)}_{\delta=0}(t)\rangle \quad . \tag{A3}$$

Since we have already shown that the eigenmode $\boldsymbol{Q}^{(+)}_\delta(t)$ is orthogonal to $\boldsymbol{v}_\nu(t)$, $\nu \neq +$ we have $\boldsymbol{Q}^{(+)}_{\delta=0}(t) = \alpha(t)\boldsymbol{u}_+(t)$ with a periodic modulation factor $\alpha(t) = \alpha(t+\tau)$. Then eq.(A3) simplifies to

$$\Gamma^{(+)}_{\delta=0}[\kappa] - \lambda_+ + \frac{\dot\alpha(t)}{\alpha(t)} = -\kappa\langle \boldsymbol{w}(t)|\boldsymbol{u}_+(t)\rangle \quad . \tag{A4}$$

Integration over one period yields eq.(21).

One may calculate the derivatives of $\Gamma^{(+)}_\delta[\kappa]$ with respect to δ and κ by standard methods of linear algebra. If we consider the adjoint eigenvalue equation

$$\Gamma^{(+)}_\delta[\kappa]\boldsymbol{P}^{(+)\dagger}_\delta(t) - \dot{\boldsymbol{P}}^{(+)\dagger}_\delta(t) = \boldsymbol{P}^{(+)\dagger}_\delta(t) D\boldsymbol{f}(\boldsymbol{\xi}(t)) - \kappa\langle \boldsymbol{P}^{(+)}_\delta(t)|\boldsymbol{u}_+(t-\delta)\rangle \boldsymbol{w}^\dagger(t-\delta), \quad \boldsymbol{P}^{(+)}_\delta(t) = \boldsymbol{P}^{(+)}_\delta(t+\tau) \quad , \tag{A5}$$

take the derivative of eq.(18) with respect to δ, and multiply with $\boldsymbol{P}^{(+)}_\delta(t)$ we obtain

$$\begin{aligned} &\partial_\delta \Gamma^{(+)}_\delta[\kappa]\langle \boldsymbol{P}^{(+)}_\delta(t)|\boldsymbol{Q}^{(+)}_\delta(t)\rangle + \frac{d}{dt}\langle \boldsymbol{P}^{(+)}_\delta(t)|\partial_\delta \boldsymbol{Q}^{(+)}_\delta(t)\rangle \\ &= \kappa\left(\langle \boldsymbol{P}^{(+)}_\delta(t)|\dot{\boldsymbol{u}}_+(t-\delta)\rangle\langle \boldsymbol{w}(t-\delta)|\boldsymbol{Q}^{(+)}_\delta(t)\rangle + \langle \boldsymbol{P}^{(+)}_\delta(t)|\boldsymbol{u}_+(t-\delta)\rangle\langle \dot{\boldsymbol{w}}(t-\delta)|\boldsymbol{Q}^{(+)}_\delta(t)\rangle\right) \quad . \end{aligned} \tag{A6}$$

Observing the periodicity and normalisation of the eigenvectors we end up with

$$\partial_\delta \Gamma^{(+)}_\delta[\kappa] = \frac{\kappa}{\tau}\int_0^\tau \langle \boldsymbol{P}^{(+)}_\delta(t)|\dot{\boldsymbol{u}}_+(t-\delta)\rangle\langle \boldsymbol{w}(t-\delta)|\boldsymbol{Q}^{(+)}_\delta(t)\rangle + \langle \boldsymbol{P}^{(+)}_\delta(t)|\boldsymbol{u}_+(t-\delta)\rangle\langle \dot{\boldsymbol{w}}(t-\delta)|\boldsymbol{Q}^{(+)}_\delta(t)\rangle \, dt \quad . \tag{A7}$$

In a similar fashion the derivative with respect to κ can be evaluated

$$\partial_\kappa \Gamma^{(+)}_\delta[\kappa] = -\frac{1}{\tau}\int_0^\tau \langle \boldsymbol{P}^{(+)}_\delta(t)|\boldsymbol{u}_+(t-\delta)\rangle\langle \boldsymbol{w}(t-\delta)|\boldsymbol{Q}^{(+)}_\delta(t)\rangle \, dt \quad . \tag{A8}$$

Taking the derivative of eq.(24) with respect to δ we obtain eq.(25) where

$$A(\delta) = -\frac{\int_0^\tau \langle \boldsymbol{P}^{(+)}_\delta(t)|\dot{\boldsymbol{u}}_+(t-\delta)\rangle\langle \boldsymbol{w}(t-\delta)|\boldsymbol{Q}^{(+)}_\delta(t)\rangle + \langle \boldsymbol{P}^{(+)}_\delta(t)|\boldsymbol{u}_+(t-\delta)\rangle\langle \dot{\boldsymbol{w}}(t-\delta)|\boldsymbol{Q}^{(+)}_\delta(t)\rangle \, dt}{\int_0^\tau \langle \boldsymbol{P}^{(+)}_\delta(t)|\boldsymbol{u}_+(t-\delta)\rangle\langle \boldsymbol{w}(t-\delta)|\boldsymbol{Q}^{(+)}_\delta(t)\rangle \, dt} \quad . \tag{A9}$$

Here $\boldsymbol{Q}^{(+)}_\delta(t)$ denotes the solution of the eigenvalue problem (18) and $\boldsymbol{P}^{(+)}_\delta(t)$ is the solution of the corresponding adjoint problem (A5) for $\kappa = 2K_{\text{fl}}(\delta)$ and $\Gamma^{(+)}_\delta[\kappa] = i\pi/\tau$. The evaluation of eq.(A9) becomes quite tedious, even in the limit of small δ. If, however, we confine attention to the special choice $\boldsymbol{w}(t) = \boldsymbol{v}_+(t)$ then eq.(A5) tells us that $\boldsymbol{P}^{(+)}_{\delta=0}(t) = \boldsymbol{v}_+(t)$. Since $\boldsymbol{Q}^{(+)}_{\delta=0}(t) = \boldsymbol{u}_+(t)$ holds (cf. eq.(18)) the normalisation (14) yields

$$A(\delta) = \mathcal{O}(\delta) \quad . \tag{A10}$$

Thus for the special choice $\boldsymbol{w}(t) = \boldsymbol{v}_+(t)$ the dependence of $K_{\text{fl}}(\delta)$ on the phase shift is according to eq.(26) of second order in δ in the exponent.

---

[1] R. Bellmann, *Introduction to the Mathematical Theory of Control Processes* (Acad. Press, New York, 1971).

[2] H. Nijmeijer and A. Schaft, *Nonlinear Dynamical Control Systems* (Springer, New York, 1996).

[3] K. Ogata, *Modern Control Engineering* (Prentince–Hall, New York, 1997).

[4] E. Ott, C. Grebogi, and Y. A. Yorke, *Controlling Chaos*, Phys. Rev. Lett. **64**, 1196 (1990).
[5] T. Shinbrot, *Progress in the control of chaos*, Adv. Phys. **44**, 73 (1995).
[6] *Handbook of Chaos Control*, edited by H. G. Schuster (Wiley–VCH, Berlin, 1999).
[7] K. Pyragas, *Continuous control of chaos by self–controlling feedback*, Phys. Lett. A **170**, 421 (1992).
[8] S. Bielawski, D. Derozier, and P. Glorieux, *Controlling unstable periodic orbits by a delayed continuous feedback*, Phys. Rev. E **49**, R971 (1994).
[9] T. Pierre, G. Bonhomme, and A. Atipo, *Controlling the chaotic regime of nonlinear ionization waves using time–delay autosynchronization method*, Phys. Rev. Lett. **76**, 2290 (1996).
[10] W. Just, T. Bernard, M. Ostheimer, E. Reibold, and H. Benner, *Mechanism of time–delayed feedback control*, Phys. Rev. Lett. **78**, 203 (1997).
[11] H. Nakajima, *On analytical properties of delayed feedback control of chaos*, Phys. Lett. A **232**, 207 (1997).
[12] J. E. S. Socolar, D. W. Sukow, and D. J. Gauthier, *Stabilizing unstable periodic orbits in fast dynamical systems*, Phys. Rev. E **50**, 3245 (1994).
[13] W. Just, D. Reckwerth, E. Reibold, and H. Benner, *Influence of control loop latency on time-delayed feedback control*, Phys. Rev. E **59**, 2826 (1999).
[14] L. Collatz, *Über Stabilität von Regelungen mit Nachlaufzeit*, ZAMM **25/27**, 60 (1947).
[15] A. Kittel, J. Parisi, and K. Pyragas, *Delayed feedback control of chaos by self–adapted delay–time*, Phys. Lett. A **198**, 433 (1995).
[16] H. Nakajima, H. Ito, and Y. Ueda, *Automatic adjustment of delay time and feedback gain in delayed feedback control of chaos*, IEICE Trans. Fund. Electr. **E80A**, 1554 (1997).
[17] W. Just, J. Möckel, D. Reckwerth, E. Reibold, and H. Benner, *Delayed feedback control of periodic orbits in autonomous systems*, Phys. Rev. Lett. **81**, 562 (1998).
[18] A. V. Mamaev and M. Saffman, *Selection of unstable patterns and control of optical turbulence by Fourier plane filtering*, Phys. Rev. Lett. **80**, 3499 (1998).
[19] R. Bellmann, *Differential–Difference Equations* (Acad. Press, New York, 1963).
[20] W. Just, E. Reibold, H. Benner, K. Kacperski, F. Fronczak, and J. Holyst, *Limits of time–delayed feedback control*, Phys. Lett. A **254**, 158 (1999).
[21] W. Just, E. Reibold, K. Kacperski, P. Fronczak, J. Holyst, and H. Benner, *Influence of stable Floquet exponents on time–delayed feedback control*, Phys. Rev. E **61**, 5045 (2000).
[22] A. Wacker and E. Schöll, *Spiking in an activator–inhibitor model for elements with S–shaped negative differential conductivity*, Z. Phys. B **93**, 431 (1994).
[23] E. Schöll, *Nonlinear spatio-temporal dynamics and chaos in semiconductors* (Cambridge University Press, Cambridge, 2001).
[24] O. Beck, A. Amann, E. Schöll, J. E. S. Socolar, and W. Just, *Comparison of time–delayed feedback schemes for spatio–temporal control of chaos in a reaction–diffusion system with global coupling*, Phys. Rev. E **66**, 016213 (2002).
[25] G. Franceschini, S. Bose, and E. Schöll, *Control of chaotic spatiotemporal spiking by time–delay autosynchronization*, Phys. Rev. E **60**, 5426 (1999).
[26] N. Baba, A. Amann, E. Schöll, and W. Just, *Giant improvement of time–delayed feedback control by spatio–temporal filtering*, Phys. Rev. Lett. **89**, 074101 (2002).
[27] H. G. Schuster and M. B. Stemmler, *Control of chaos by oscillating feedback*, Phys. Rev. E **56**, 6410 (1997).
[28] W. Just, *On the eigenvalue spectrum for time–delayed Floquet problems*, Physica D **142**, 153 (2000).
[29] S. Bielawski, D. Derozier, and P. Glorieux, *Experimental characterization of unstable periodic orbits by controlling chaos*, Phys. Rev. A **47**, R2492 (1993).
[30] J. K. Hale and S. M. Verduyn Lunel, *Introduction to Functional Differential Equations* (Springer, New York, 1993).
[31] G. Benettin, L. Galgani, A. Giorgilli, and J. Strelcyn, *Lyapunov characteristic exponents for smooth dynamical systems: method for computing them all*, Meccanica **15**, 9&21 (1980).
[32] M. E. Bleich and J. E. S. Socolar, *Controlling spatiotemporal dynamics with time–delayed feedback*, Phys. Rev. E **54**, R17 (1996).